Thermal and photoinduced liquid crystalline phase transitions with a rod-disc alternative change in the molecular shape

Daisuke Tanaka, Hisato Ishiguro, Yo Shimizu and Kingo Uchida**

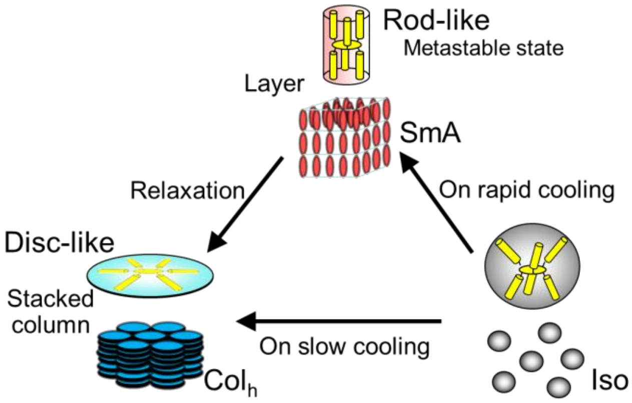

Figure S1 Kinetically controlled monotropic liquid crystalline (LC) phases observed in **1-C10**.[1] The faster cooling (5 °C min^{-1}) makes the molecules form an SmA phase (calamitic system), while the slower cooling (1 °C min^{-1}) gives a Col$_h$ phase (discotic system).

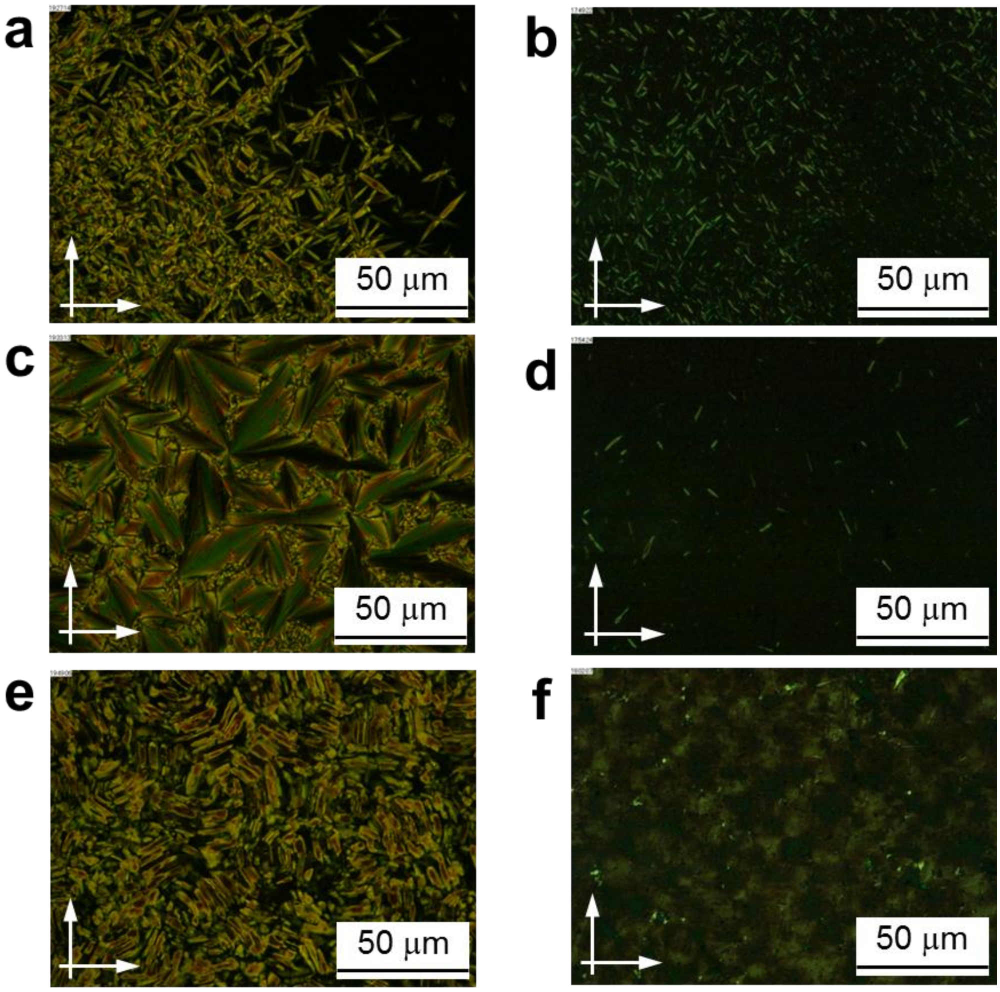

Figure S2. Optical texture change at the phase transitions of compound **1-C14** in a homogeneous orientation (a, c, and e) and a homeotropic orientation (b, d, and f). a-b) “Bâtonnets” texture arises at 209.8 °C, c) fan-shaped texture is formed by the growth of “bâtonnets” and e-f) the optical texture changes at 203.1 °C corresponding to the SmA-to-Col_r mesophase on cooling. The arrows indicate the polarizing direction of the analyzer and polarizer. (Scale bar: 50 μm)

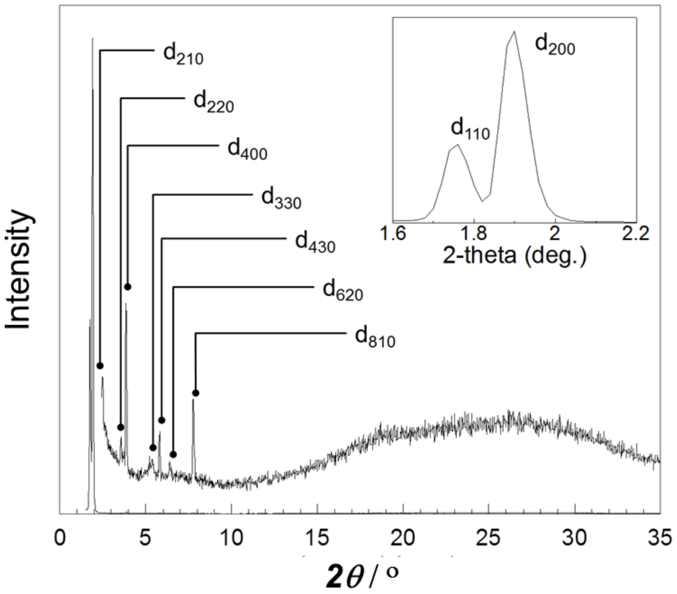

Figure S3. XRD patterns for non-aligned samples at 200 °C. The set of reflections emerging in the small angle region corresponds to the 2-dimentional lattice of a columnar array, and there is indication of stacking periodicity within a column, which is expected at ca. 3.5 Å where one can see a broad halo derived from the molten alkyl chains centered at ca. 4.5 Å.

Table S1. Observed and calculated *d*-spacing of the observed XRD of P2/a phase in compound **1-C14** at 200 °C (Fig. S3).

(hkl)	$d_{obs.}$-spacing (Å)	$d_{cal.}$-spacing (Å)
(110)	50.2	50.2
(200)	46.5	46.5
(210)	35.9	36.6
(220)	24.8	25.1
(400)	23.0	23.2
(330)	16.6	16.7
(430)	15.2	15.1
(620)	13.8	13.7
(810)	11.4	11.4
br	4.8	
(001)	3.4	
a= 92.9 Å, *b*= 59.6 Å		

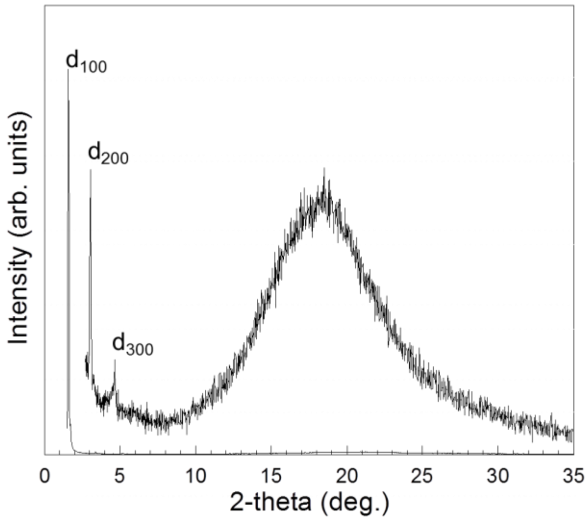

Figure S4. XRD pattern of compound **1-C14** at 207 °C

Table S2. Observed and calculated *d*-spacing of the observed XRD of SmA phase in compound **1-C14** at 207 °C (Fig. S4).

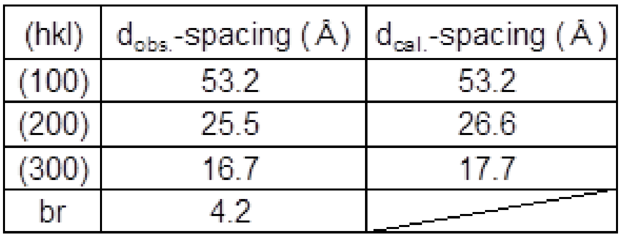

(hkl)	d$_{obs.}$-spacing (Å)	d$_{cal.}$-spacing (Å)
(100)	53.2	53.2
(200)	25.5	26.6
(300)	16.7	17.7
br	4.2	

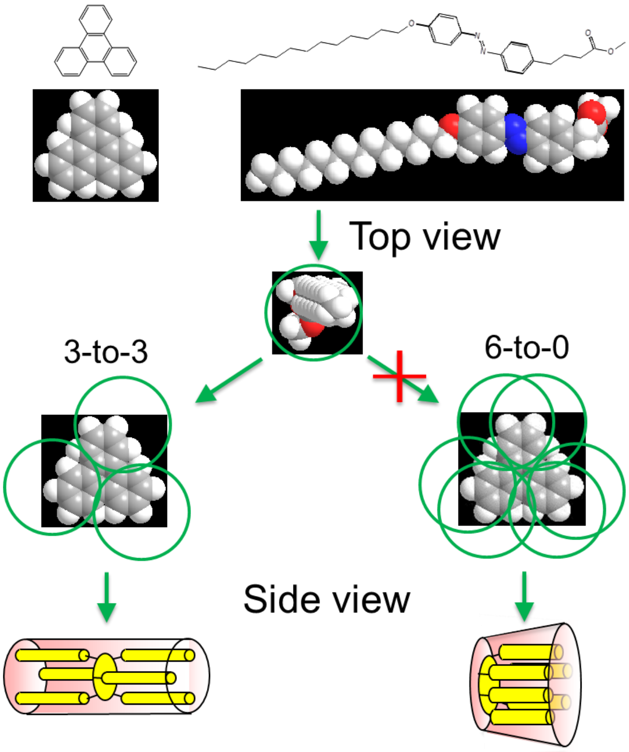

Figure S5. Schematic illustrations of the rod-like molecular shapes in calamitic LC state. (Each molecular part was optimized by using of Gaussian RHF/3-31G)

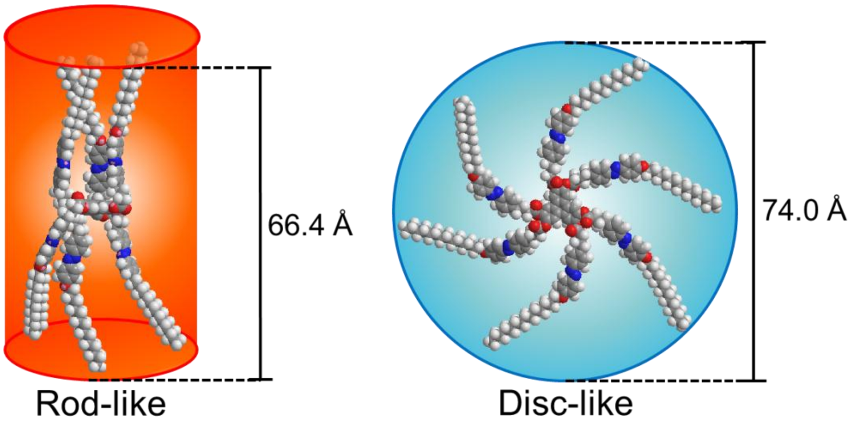

Figure S6. The molacular diameter and length of disc- and rod-like comformation of **1-C14** with Chem3D.

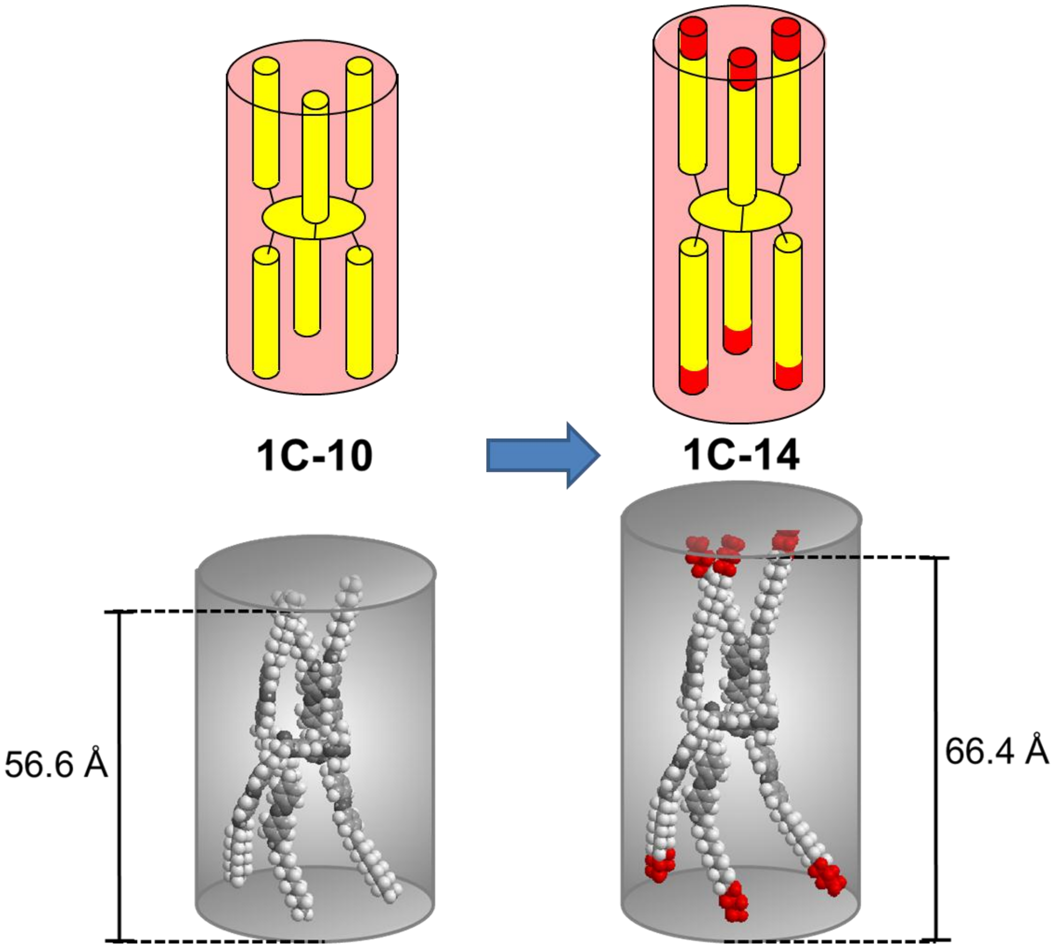

Figure S7. Stabilization of smectic A phase by elongation of the terminal alkyl groups

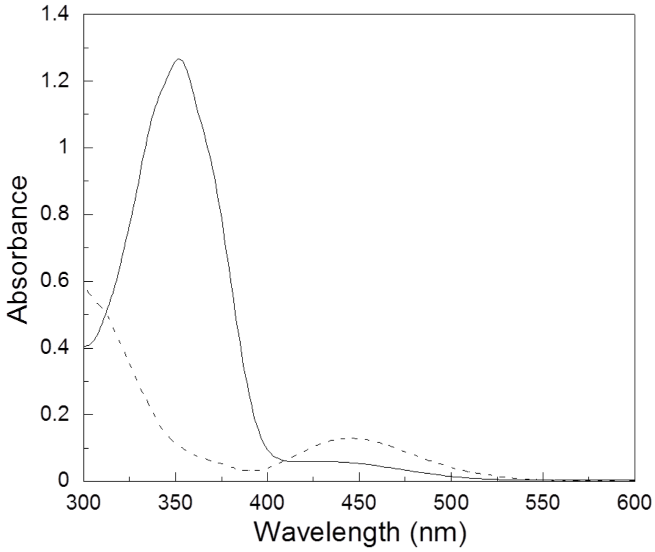

Figure S8. Absorption spectral changes of **1-C14** in toluene solution (2.6 × 10^{-5} mol L^{-1}). Solid line: before UV irradiation, Dotted line: after UV (365 nm) irradaition.

The absorption spectrum of trans-form of **1-C14** shows the absorption maximum at 352 nm (4.8 × 10^{4} $M^{-1}cm^{-1}$). Upon UV irradiation the band decreased with increasing the new band at 446 nm attributed to nπ* of *cis*-isomer of azobenzene moieties. It reverted to the original one in the dark.

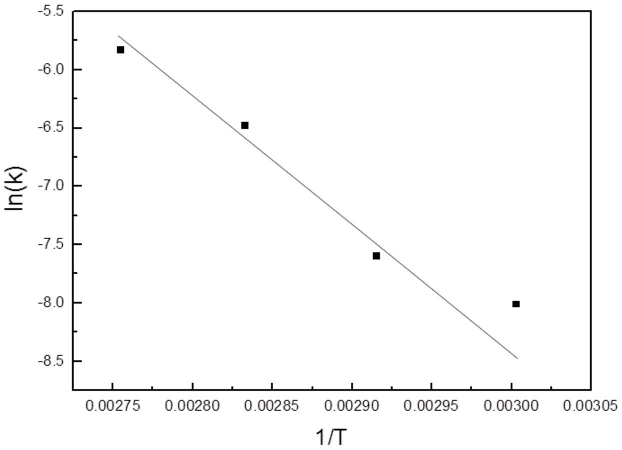

Figure S9. Activation energy of thermal *cis* to *trans* isomerization of the azobenzene moieties of **1C-14.** The decay rates were measured by monitoring the thermal decay of the absorbance at 444 nm attributed to the cis-azobenzene at 60, 70, 80 and 90°C, and the activation energy was obtained to be 91.8 kJ/mol according to the Arrhenius equation.

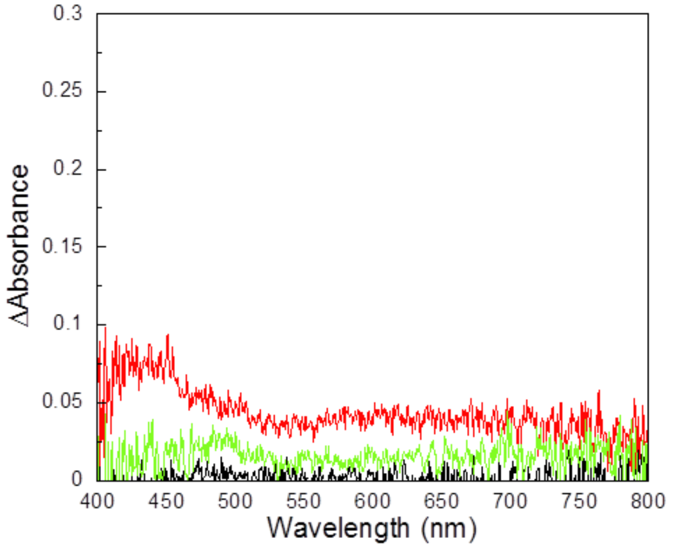

Figure S10. Transient absorption spectra of **1-C14** in liquid crystalline state at 200 °C after irradiation of Q switched laser pulse. Laser pulse was irradiated through the hotstage (METLLER, FP82HT hot stage) keeping the temperature. After the excitation of the nanosecond 355 nm laser pulse (THG of Quanta-Ray, DCR-3 Nd^{3+}:YAG laser, with an intensity of 3-5 mJ / pulse), transient spectra were monitored with a polychromator (Acton, M4197, The setup of the system is shown in Fig. S10). Black line shows spectrum before laser pulse irradiation. The band attributed to the *cis*-isomer of **1-C14** around 450 nm was observed after 50 ns (red line) indicating the formation of *cis*-isomer even at 200 °C (The broad band around 600-800 nm is due to the diffraction attributed to the phase transition of LC phases). The spectrum after 100 μs is indicated green line which strongly suggest the lifetime of *cis*-isomer at 200 °C is μs order.

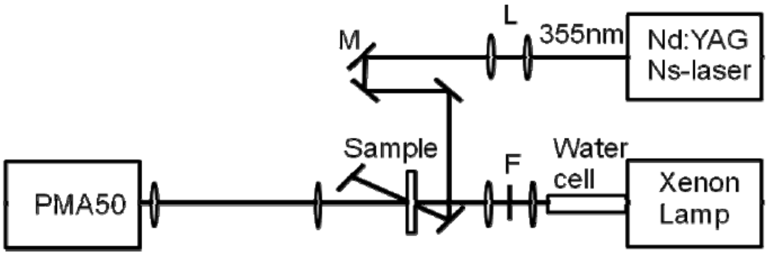

Figure S11. Schematic of laser-probe transient absorption apparatus: 355-nm pump laser (Nd:YAG), Photo-Multichannel-Analyzer-50 (PMA50), mirror (M), filter (F), and lens(L). Beam diameter was changed by two focus lenses (100 mm and 50 mm, respectively). Water cell was placed in front of Xenon lamp to prohibit the thermal effect.

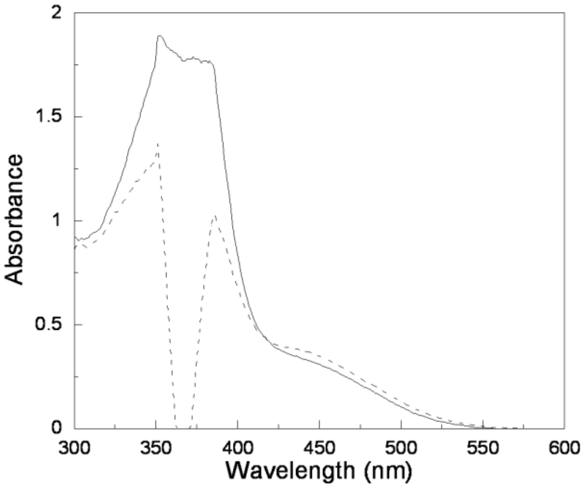

Figure S12. Absorption spectral changes of the bulk film of **1-C14** at 200 °C by a reflection absorption spectroscopy. Solid line: before UV irradiation; dotted line: during the 365 nm light irradiation with 1 Wcm^{-2}. Enhancement of the band around 450 nm due to the n-π* band of *cis*-azobenzene moiety was observed. The hollow at 365 nm is due to the reflection of the incident light.

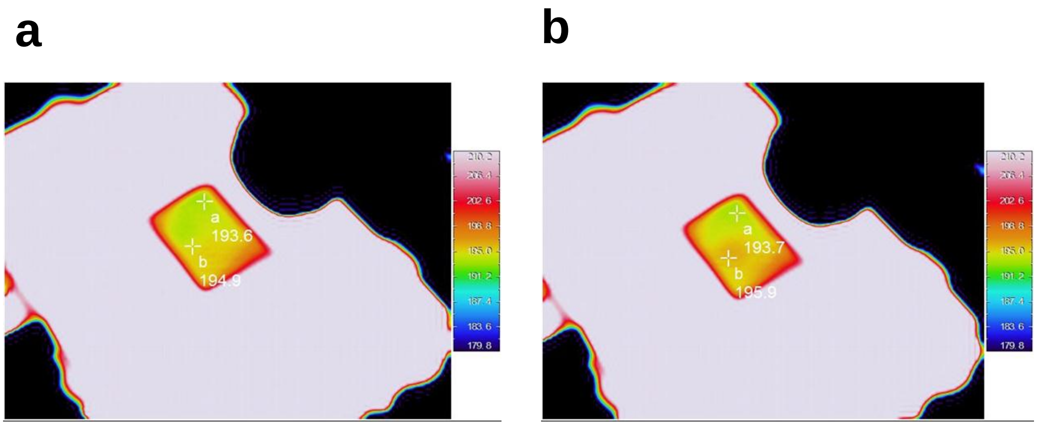

Figure S13. Thermographic pictures without UV irradiation (a) and under UV irradiation (b) by 365 nm (1.0 Wcm^{-2}) to the center part of the bulk film of **1-C14** on the glass substrate. Temperature of the (Mettler FP90) processor controlling the hotstage (Mettler FP82HT) under the film was set at 200°C. The pictures were taken on a hotstage with keeping the cover opened and without cover glass. The color bar right side indicates the temperatures. Only 1°C of enhancement was observed at point b (irradiated site by the90 light souse applied in LC phase changes) in the thermogram (b).

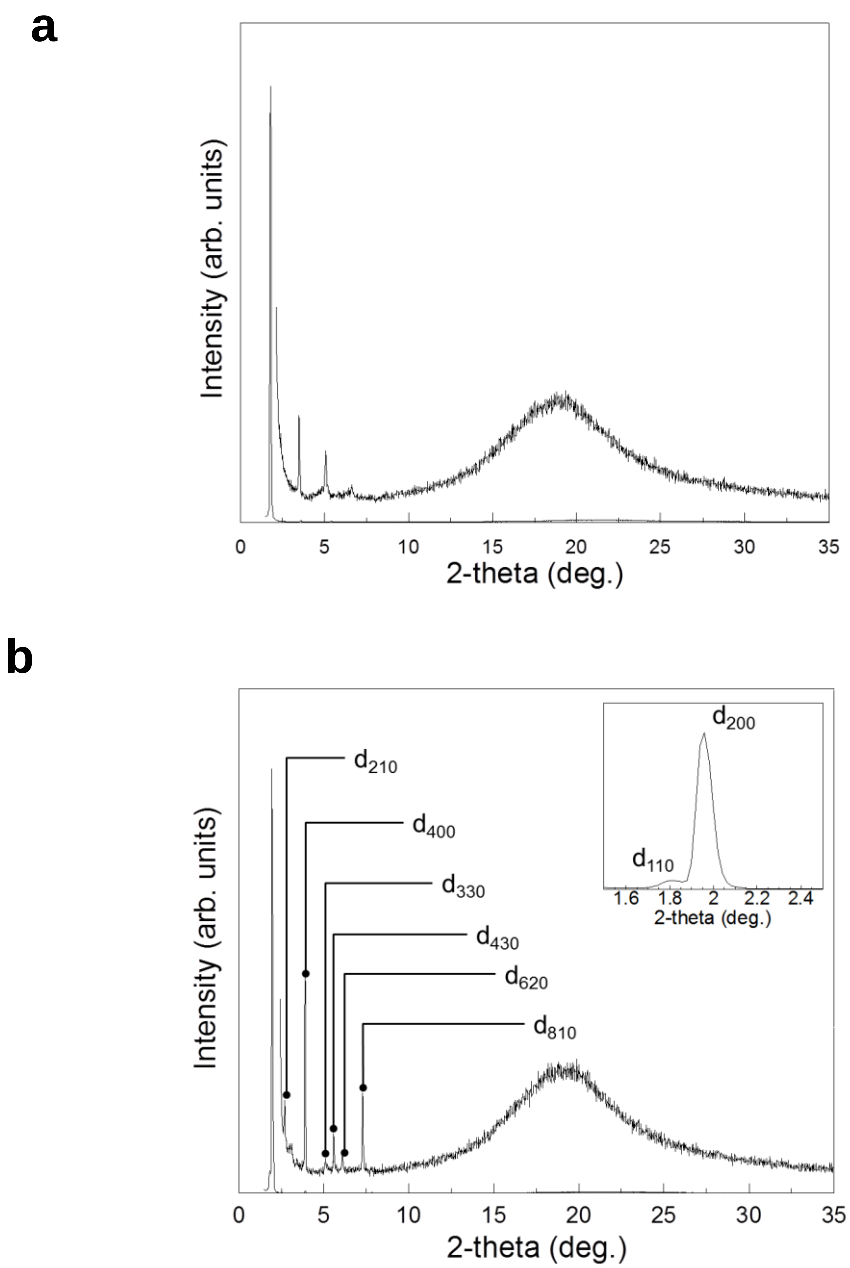

Figure S14. XRD patterns of compound **1-C14** under UV irradiation (365 nm; 0.5 W / cm^{-2}) at 204 °C (a), and at 197 °C (b).

Table S3. Observed and calculated *d*-spacing of the observed XRD of SmA phase in compound **1-C14** under UV irradiation (365nm; 0.5 W / cm^{-2}) at 204 °C (Fig. S14a).

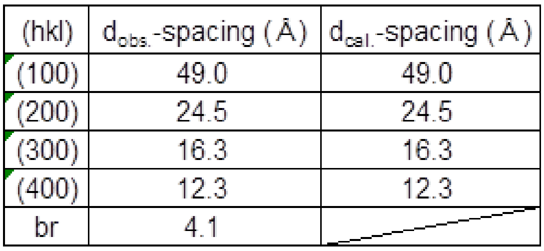

(hkl)	$d_{obs.}$-spacing (Å)	$d_{cal.}$-spacing (Å)
(100)	49.0	49.0
(200)	24.5	24.5
(300)	16.3	16.3
(400)	12.3	12.3
br	4.1	

Table S4. Observed and calculated *d*-spacing of the observed XRD of P2/a phase in compound **1-C14** under UV irradiation (365nm; 0.5 W / cm^{-2}) at 197 °C (Fig. S14b).

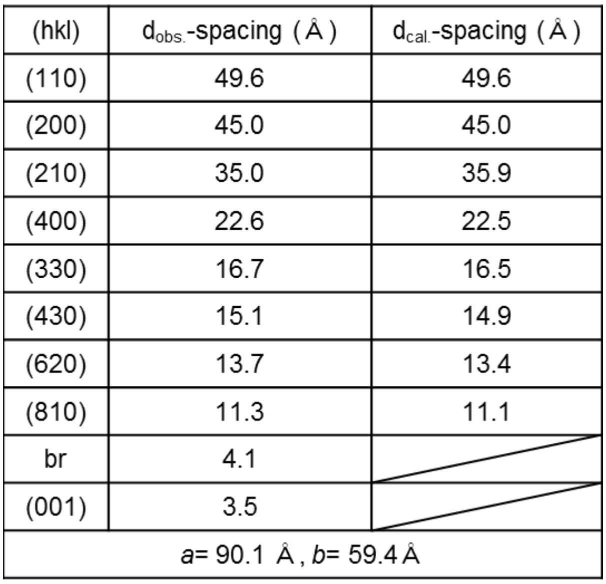

(hkl)	$d_{obs.}$-spacing (Å)	$d_{cal.}$-spacing (Å)
(110)	49.6	49.6
(200)	45.0	45.0
(210)	35.0	35.9
(400)	22.6	22.5
(330)	16.7	16.5
(430)	15.1	14.9
(620)	13.7	13.4
(810)	11.3	11.1
br	4.1	
(001)	3.5	
a= 90.1 Å , *b*= 59.4 Å		

The distance between the layers of SmA phase was decreased from 53.1 to 49.0 Å (Tables S2 and S3) and lattice constant *a* for Col$_r$ phase was also reduced from 92.92 to 90.06 Å upon UV irradiation (Tables S1 and S4). These results indicate that the linearity of the azobenzene moieties reduced by the *trans-cis* isomerization.

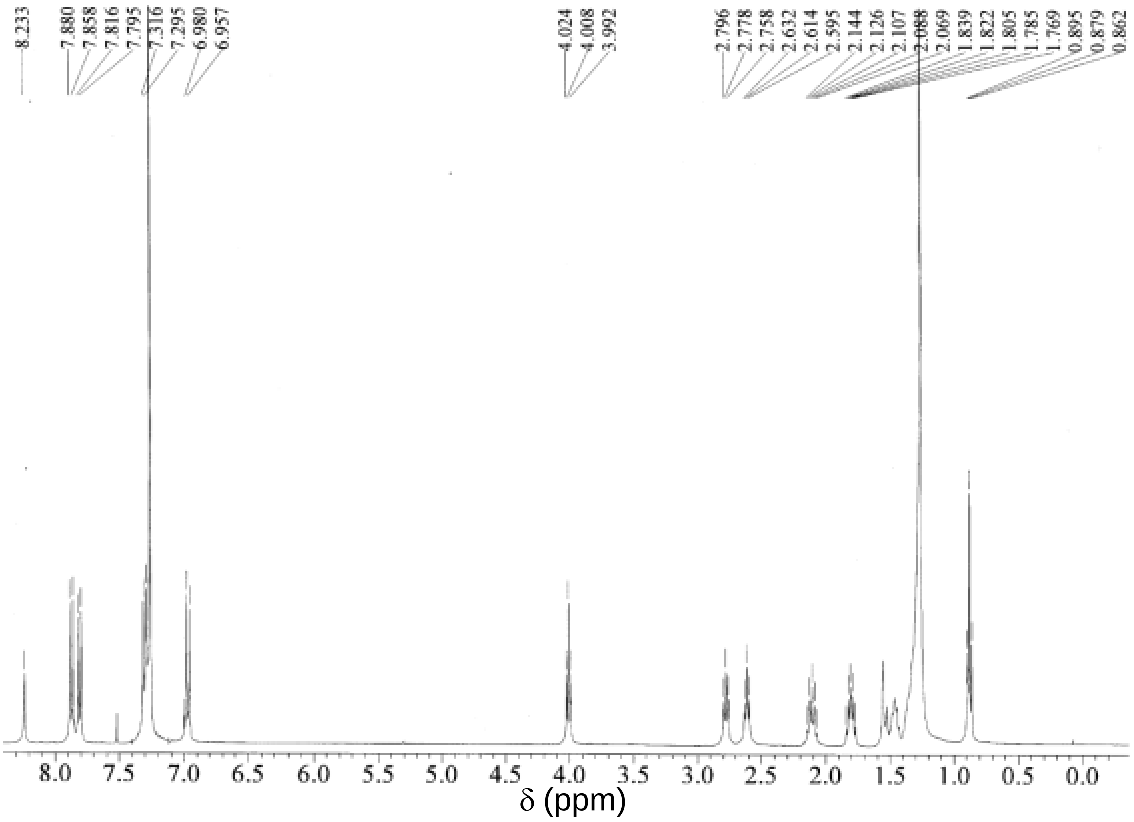

Figure S15. ^{1}H NMR spectrum of compound **1-C14**

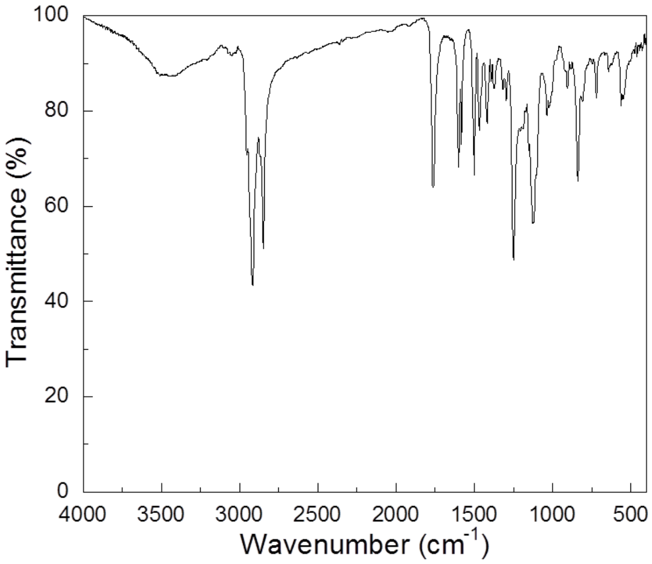

Figure S16. IR spectrum of compound **1-C14**

Reference

[1] Y. Shimizu, A. Kurobe, H. Monobe, N. Terasawa, K. Kiyohara, and K. Uchida, *Chem. Commun.* 2003, 1676-1677.